445. Combinatorial Antiangiogenic Gene Therapy by Nonviral Gene Transfer Using the Sleeping Beauty Transposon Causes Tumor Regression and Improves Survival in Mice Bearing Intracra…

Article *in* Molecular Therapy · December 2005

DOI: 10.1016/j.ymthe.2005.07.689 · Source: PubMed

CITATIONS
128

READS
108

12 authors, including:

Zachary L Demorest
University of Minnesota Twin Cities
32 PUBLICATIONS **1,687** CITATIONS
SEE PROFILE

Seunguk Oh
University of Minnesota Twin Cities
22 PUBLICATIONS **951** CITATIONS
SEE PROFILE

Eleanor Chen
University of Washington Seattle
123 PUBLICATIONS **2,160** CITATIONS
SEE PROFILE

Stephen Carl Ekker
Mayo Foundation for Medical Education and Research
405 PUBLICATIONS **16,244** CITATIONS
SEE PROFILE

ARTICLE

doi:10.1016/j.ymthe.2005.07.689

Combinatorial Antiangiogenic Gene Therapy by Nonviral Gene Transfer Using the *Sleeping Beauty* Transposon Causes Tumor Regression and Improves Survival in Mice Bearing Intracranial Human Glioblastoma

John R. Ohlfest,[1] Zachary L. Demorest,[1] Yasuhiko Motooka,[1] Isabelita Vengco,[1] Seunguk Oh,[1] Eleanor Chen,[2] Frank A. Scappaticci,[3] Rachel J. Saplis,[2] Stephen C. Ekker,[2] Walter C. Low,[1] Andrew B. Freese,[1] and David A. Largaespada[2,*]

[1]*Department of Neurosurgery, University of Minnesota, Minneapolis, MN 55455, USA*
[2]*Department of Genetics, Cell Biology, and Development, University of Minnesota Cancer Center, and the Arnold and Mabel Beckman Center for Transposon Research, Minneapolis, MN 55455, USA*
[3]*Department of Internal Medicine, University of California Davis Cancer Center, Sacramento, CA 95817, USA*

**To whom correspondence and reprint requests should be addressed at the Department of Genetics, Cell Biology, and Development, University of Minnesota, 6-160 Jackson Hall, 321 Church Street SE, Minneapolis, MN 55455, USA. E-mail: larga002@tc.umn.edu.*

Available online 16 September 2005

Glioblastoma is a fatal brain tumor that becomes highly vascularized by secreting proangiogenic factors and depends on continued angiogenesis to increase in size. Consequently, a successful antiangiogenic therapy should provide long-term inhibition of tumor-induced angiogenesis, suggesting long-term gene transfer as a therapeutic strategy. In this study a soluble vascular endothelial growth factor receptor (sFlt-1) and an angiostatin–endostatin fusion gene (statin-AE) were codelivered to human glioblastoma xenografts by nonviral gene transfer using the *Sleeping Beauty* (SB) transposon. In subcutaneously implanted xenografts, co-injection of both transgenes showed marked anti-tumor activity as demonstrated by reduction of tumor vessel density, inhibition or abolition of glioma growth, and increase in animal survival ($P = 0.003$). Using luciferase-stable engrafted intracranial gliomas, the anti-tumor effect of convection-enhanced delivery of plasmid DNA into the tumor was assessed by luciferase *in vivo* imaging. Sustained tumor regression of intracranial gliomas was achieved only when statin-AE and sFlt-1 transposons were coadministered with SB-transposase-encoding DNA to facilitate long-term expression. We show that SB can be used to increase animal survival significantly ($P = 0.008$) by combinatorial antiangiogenic gene transfer in an intracranial glioma model.

Key Words: sleeping beauty, transposon, angiogenesis, glioblastoma, nonviral

INTRODUCTION

Glioblastoma multiforme (GBM) is an incurable brain tumor that usually causes death within 2 years after conventional therapies consisting of surgery, radiation, and chemotherapy [1]. Novel therapies are needed that have minimal toxicity, yet have long-lasting anti-tumor effects to avoid relapse after surgical resection. GBM is one of the most highly vascularized human tumors and is therefore an attractive target for antiangiogenic therapy [2–4]. After surgical resection, the remaining migratory tumor cells may parasitize existing vasculature, but ongoing angiogenesis occurs when tumors reach a certain size threshold [5]. Thus, if the net concentration of antiangiogenic factors could be increased long term, the regrowth of gliomas could be stunted.

We favor delivery of angiogenic inhibitors by gene transfer rather than systemic administration because gene transfer can facilitate sustained levels of inhibitor at the tumor site [6–8], where proangiogenic factors are continuously released [2,3]. Accordingly, it is not surprising that the initial clinical trials that relied on systemic administration of antiangiogenic proteins showed little, if any, anti-tumor effect [9,10]. Recent studies suggest that coadministration of multiple inhibitors of angiogenesis that act by different mechanisms increases the efficacy of antiangiogenic therapy [11–14], much like combinatorial chemotherapy shows synergistic anti-

1525-0016/$30.00

tumor effects [15–17]. The current study supports this hypothesis.

To meet the demand for a tumor-gene-transfer vector that is amenable to large-scale manufacture and can achieve sustained gene expression, we previously developed plasmid-based vectors capable of integration and long-term expression in xenografted human glioblastoma [18]. Our plasmid vectors are capable of transgene integration and long-term expression using the *Sleeping Beauty* (SB) transposable element, a cut-and-paste transposon of the *Tc1/mariner* superfamily [18,19]. The SB transposase enzyme catalyzes integration of the transposon into genomic DNA [19,20]. The gene that encodes the SB transposase enzyme can be provided on a separate plasmid (*in trans*) or the same plasmid (*in cis*) relative to the transposon. SB is a promising plasmid-based gene transfer system because it facilitates long-term gene expression [21–24], even in mitotic tissue such as tumors [18], yet also avoids many of the disadvantages associated with viral vectors.

In this study we assess the anti-tumor activity of SB transposon vectors that encode two potent antiangiogenic proteins, a soluble vascular endothelial growth factor receptor (sFlt-1 [25,26]) and an angiostatin–endostatin fusion protein (statin-AE [13]). When we injected sFlt-1 and statin-AE plasmid DNA/polyethylenimine (PEI) complexes directly into GBM xenografts, we observed marked anti-tumor activity as demonstrated by reduced tumor vessel density, inhibition of tumor growth, and tumor elimination in up to 50% of nude mice. This is the first demonstration that nonviral gene transfer to experimental human glioblastoma can increase animal survival and induce complete and sustained tumor regression.

RESULTS

Nonviral Gene Transfer of sFlt-1 and Statin-AE Inhibits Glioma Growth and Tumor-Induced Angiogenesis

We constructed transposon expression vectors for sFlt-1 and statin-AE by cloning the respective cDNA under the control of a chimeric CMV enhancer/chicken β-actin promoter ("CAG promoter" [27,28]; Fig. 1A). We verified protein expression of statin-AE and sFlt-1 by an endostatin or sFlt-1 ELISA. We detected statin-AE and sFlt-1 in the cell culture lysates and in the culture supernatants, thereby demonstrating that gene transfer of these plasmids results in secretion of the statin-AE and sFlt-1 proteins from glioma cells (Figs. 1B and 1C).

To assess the effects of statin-AE and sFlt-1 gene transfer on preestablished gliomas, we gave nude mice subcutaneous tumors by injection of U373 MG cells.

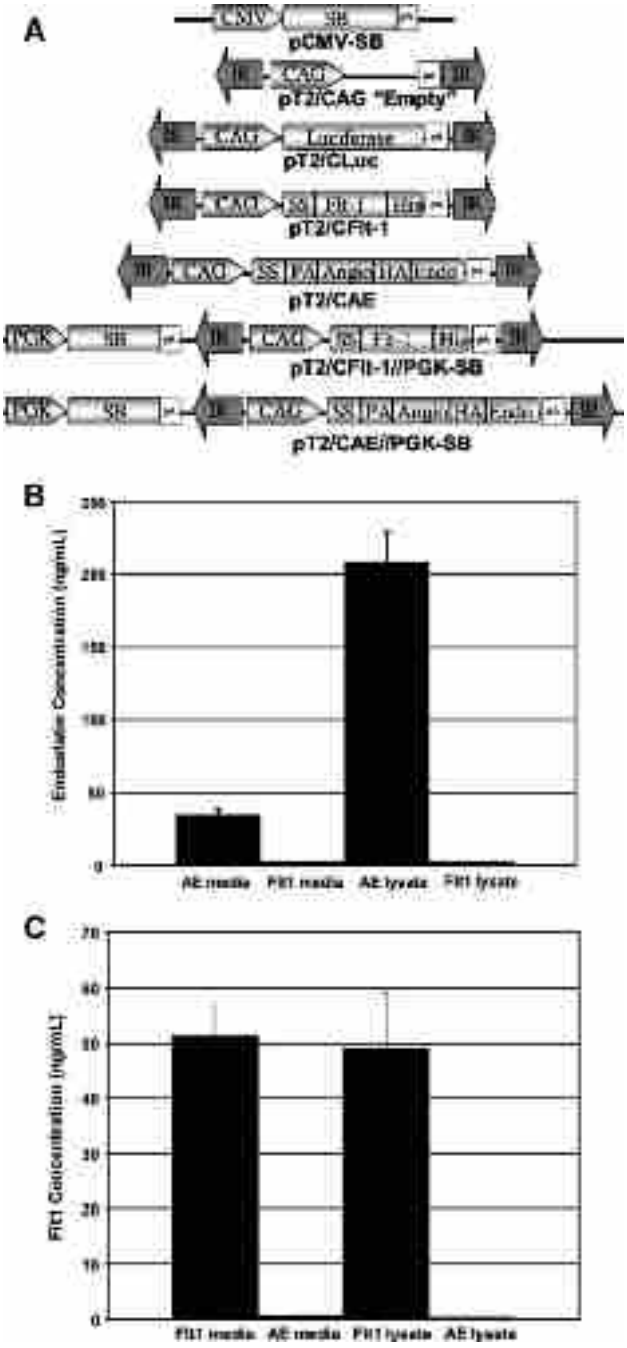

FIG. 1. Plasmid vectors and expression *in vitro.* (A) Transposon vectors all have an identical ColE1/AMPr backbone that is flanked by two inverted repeat/direct repeat elements (IR) that form the termini of the integrating unit. Expression of luciferase, statin-AE, and sFlt-1 transgenes is regulated by a chimeric cytomegalovirus (CMV) enhancer/chicken β-actin (CAG) promoter. Statin-AE is an angiostatin–endostatin fusion protein linked by an HA tag. The secretory signal (SS) for statin-AE is the native murine plasminogen SS, followed by the 3′ preactivation peptide from murine plasminogen; endostatin is also the murine version (collagen XVIII fragment) [13]. sFlt-1 is a soluble VEGF receptor that lacks the transmembrane domain, has the native murine Flt-1 SS, and has a C-terminal 6× His tag [26]. CMV or phosphoglycerate kinase (PGK) promoter elements regulate SB transposase expression. (B) Endostatin was detected by ELISA only in media or lysates from cells transfected with pT2/CAE. (C) sFlt-1 was detected by ELISA only in media or lysates from cells transfected with pT2/CFlt-1.

doi:10.1016/j.ymthe.2005.07.689

When the tumors averaged 50 mm^3 in volume, we administered 20 μg of pT2/C-AE or pT2/C-Flt-1 or empty vector (control) with 1 μg of pCMV-SB by intratumoral co-injection as plasmid DNA/PEI complexes (n = 5/group). Identical injections were repeated 3 days later for a total of two injections per tumor (Fig. 2A).

Gene transfer of statin-AE and sFlt-1 had marked anti-tumor activity as demonstrated by a significant reduction in tumor vessel density (Fig. 2B) and inhibition of tumor growth (Fig. 2A). Intratumoral administration of antiangiogenic plasmids resulted in 84 (sFlt-1-treated) and 80% (statin-AE-treated) inhibition of tumor growth by 7 weeks after plasmid injection, relative to tumors treated with noncoding plasmid. This difference was significant ($P \leq 0.03$; Fig. 2A). There was no significant difference between the anti-tumor activity of sFlt-1 and that of statin-AE (P =

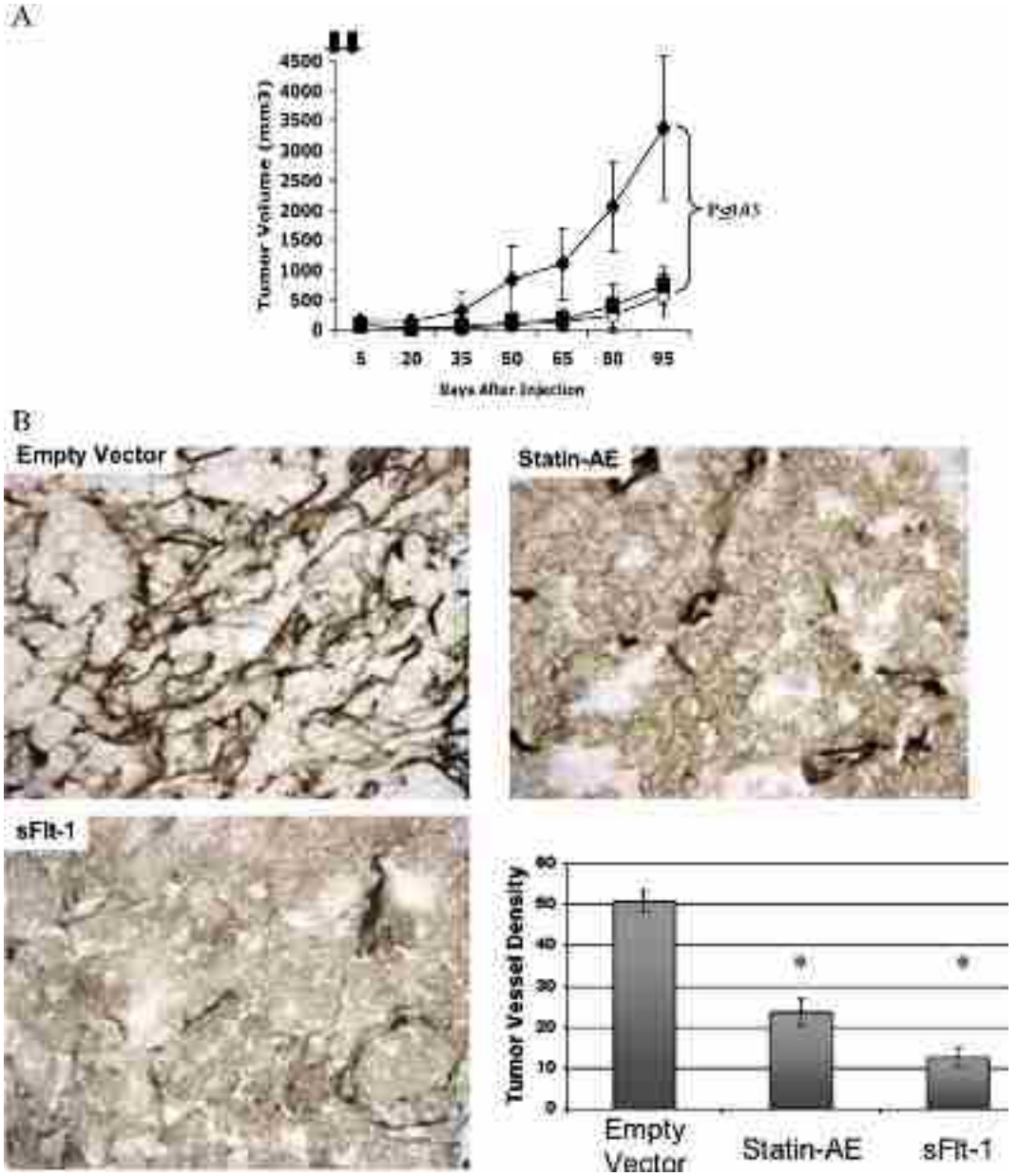

FIG. 2. (A) Mice bearing subcutaneous glioma xenografts were given two intratumoral co-injections of 1 μg pCMV-SB with 20 μg pT2/CAG (empty vector control (♦)) or pT2/CAE (■) or pT2/CFlt-1 (○) (n = 5/group). Plasmid injections were administered on day 0 and day 3 (arrows). (B) The experiment in (A) was repeated. CD31 (endothelial cell marker) immunohistochemistry was performed on the tumor cryosections 50 days after the last intratumoral injection. Three tumors that were treated with empty vector, statin-AE, or sFlt-1 were stained (three sections/tumor). *$P \leq 0.05$ compared to empty vector-treated tumors.

0.3; Fig. 2A). To determine if the therapeutic effect from gene transfer was due to inhibition of tumor-induced angiogenesis, we conducted CD31 immunohistochemistry (endothelial cell marker) on tumor cryosections to assess vessel density. We stained three tumors that were treated with empty vector, statin-AE, or sFlt-1 (three sections/tumor) and determined the average vessel density. A significant reduction in vessel density was apparent in tumors that were treated with statin-AE or sFlt-1 relative to empty vector (Fig. 2B; $P \leq 0.05$). There was no significant difference in vessel density between statin-AE and sFlt-1-treated tumors ($P = 0.48$). These data indicate that statin-AE and sFlt-1 inhibit glioma growth, at least in part, by inhibiting tumor-induced angiogenesis. This observation concurs with previous studies that used these molecules for cancer gene therapy [13,26,29].

Combinatorial Effects of Statin-AE and sFlt-1 Expression Abolished Tumorigenicity of Glioma Cells

To investigate whether simultaneous expression of statin-AE and sFlt-1 exerts synergistic anti-tumor activity, we generated stable U373 MG cell lines that expressed statin-AE and sFlt-1 alone or in combination or an empty vector control. Expression of statin-AE and sFlt-1 was confirmed by ELISA (not shown). The growth rates of these cell lines were not significantly different *in vitro* ($P \geq 0.2$ in the comparison of any combination of cell lines; Fig. 3A). We injected nude mice subcutaneously (sc) with each cell line and measured tumor growth for 6 weeks ($n = 5$/group). Stable expression of statin-AE and sFlt-1 significantly reduced the growth of tumor compared to the empty vector control cells, which formed rapidly growing tumors ($P \leq 0.05$; Fig. 3B). However, simultaneous expression of statin-AE and sFlt-1 completely blocked the ability of these human glioma cells to form tumors *in vivo* (Fig. 3B). We repeated the experiment for confirmation with nearly identical results (not shown). These studies indicate that simultaneous expression of statin-AE and sFlt-1 has greater anti-tumor activity than either protein alone.

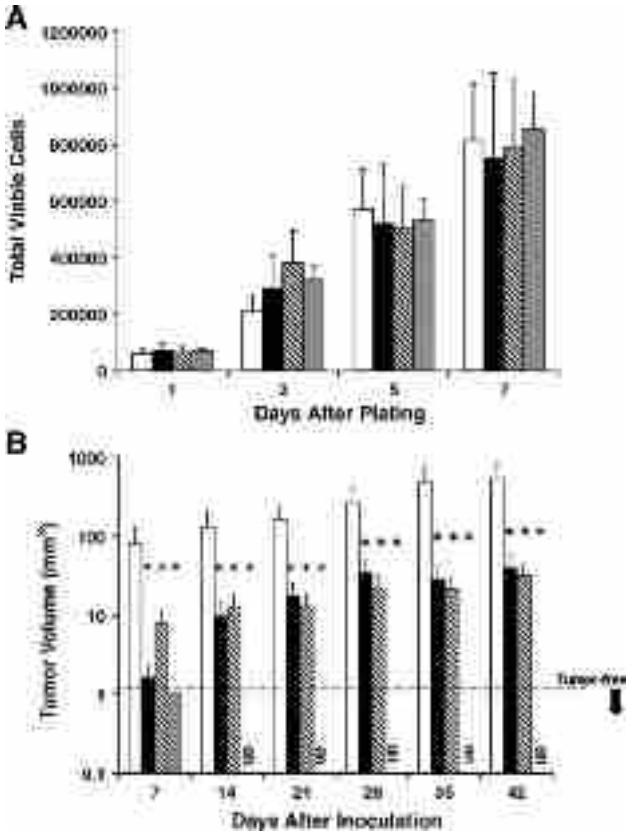

FIG. 3. (A) Stable U373 MG cells were made with pT2/CBSD and pT2/C-Hygro (empty vector control; white bar) or pT2/CAE/BSD (black bar) or pT2/CFlt-1/Hygro (striped bar) or pT2/CAE/BSD and pT2/CFlt-1/Hygro (gray bar). 50,000 cells of each stable cell line were seeded on day 0 ($n = 12$/cell line). At days 1, 3, 5, and 7 after seeding each stable cell line was counted in triplicate. The average counts are shown. (B) Nude mice were inoculated sc with each stable line (in A) or with an empty vector control line ($n = 5$/group). Tumor growth was measured weekly with calipers for 6 weeks (UD, undetectable/invisible tumor to naked eye; P value derived from Student's t test, means ± SD, $^P \leq 0.05$, $*P \leq 0.005$).

Statin-AE/sFlt-1 Combinatorial Gene Cocktail and SB-Mediated Gene Transfer Achieve Maximum Anti-tumor Effect and Prevent Tumor Relapse

We repeated the sc tumor gene transfer study with several modifications in the experimental design. First, to confirm that all tumors received successful gene transfer, we co-injected 5 μg of a luciferase-encoding plasmid with every intratumoral injection. We then imaged the animals *in vivo* for luciferase activity to assess the resultant gene transfer. Second, in an attempt to increase the anti-tumor efficacy, we coadministered statin-AE- and sFlt-1-encoding plasmids. Third, we included a non-SB-treated control to determine what contribution the transposase makes toward tumor inhibition. We established U87 MG tumors by sc inoculation and gave nude mice two intratumoral co-injections of 5 μg pT2/CLuc with 7.5 μg of pT2/CAE//PGK-SB, pT2/CFlt-1//PGK-SB, or pT2/CAE and pT2/Cflt-1 (no SB control) or an empty vector control as detailed in Fig. 4A ($n = 6$/group).

All tumors that were injected with DNA/PEI complexes had detectable luciferase expression 48 h after the intratumoral injection. There was no statistically significant difference in luciferase expression between the three treatment groups ($P \geq 0.20$; not shown), indicating that reproducible gene transfer to the tumor was achieved. Further, two intratumoral injections that included luciferase-encoding DNA in the PEI complex resulted in a level of measured luciferase activity comparable to what has been achieved with a lentivirus [30]. We measured up to 5.6×10^5 photons/s/cm^2 by injecting only 5 μg of luciferase DNA twice (Fig. 4E). These data confirm that intratumoral injection of DNA/PEI complexes is a reliable and effective nonviral means to achieve gene transfer to xenografted gliomas.

doi:10.1016/j.ymthe.2005.07.689

Empty vector-treated tumors rapidly grew and resulted in morbidity in 6/6 mice by 7 weeks after plasmid administration (Fig. 4A). In contrast, we observed a strong anti-tumor effect after administering two injections of statin-AE/sFlt-1-encoding DNA, with or without SB-transposase-encoding DNA, compared to empty vector controls. Treatment with statin-AE/sFlt-1-encoding plasmid DNA resulted in rapid regression of tumors to a size that was invisible to the naked eye in 4/6 non-SB-treated mice and 3/6 SB-treated mice. However, 3/4 tumors that regressed, and had not been treated with SB-transposase-encoding DNA, eventually regrew and killed the animals (Fig. 4B). In contrast, every tumor that regressed and that was treated with SB did not recur and the animals remained tumor-free for 200 days (Fig. 4C). Coadministration of SB-transposase-encoding DNA with the statin-AE/sFlt-1 transposon vectors resulted in the highest level of long-term survivors (50%; $P < 0.005$) relative to non-SB-treated animals (17%; $P = 0.03$) or empty vector (0%; Fig. 4D). This study reveals that SB-mediated gene transfer of antiangiogenic transposon vectors induces long-lasting anti-tumor effects.

A Luciferase-Stable Glioma Cell Line Allows Noninvasive Assessment of Tumor Burden for Improved Reliability and Relevance of the Intracranial Glioma Model

Many studies use intracranial glioma models in which treatment by toxin or gene therapy begins before the injected-tumor cells have formed an appreciable tumor mass [6,31,32] and therefore may not be an ideal model for a large human glioma. In addition, we have found significant variability in the growth rate of intracranial tumor xenografts even when the identical cell dose is injected into the same coordinates (Fig. 5A). To improve the reliability and relevance of our intracranial glioma model, we engineered U87 MG cells to express firefly luciferase stably so that luciferase *in vivo* imaging could be used to quantify tumor burden [33].

We imaged mice bearing intracranial luciferase-stable tumors for luciferase activity and then euthanized them to analyze the size of the tumor at light intensities of 10^5, 10^6, and 10^7 photons/s/cm^2 (psc). A light intensity of 10^5 psc corresponded to a tumor that was approximately 1 mm^3 in volume, 10^6 psc to 30 mm^3 in volume, and 10^7 psc to 74 mm^3 in volume (Fig. 5B). Mice injected with the same dose of cells had tumors that grew at different rates (Fig. 5A). We conclude that *in vivo* imaging of luciferase-stable tumor cells provides an easy method to quantify intracranial tumor burden. This approach could be used to standardize future studies by treating tumors of the same size, rather than treating all animals at the same time after tumor inoculation.

Convection-Enhanced Delivery of a Statin-AE/sFlt-1/SB Gene Cocktail to Intracranial Human Glioblastoma Significantly Improved Animal Survival and Caused Complete Tumor Regression

We treated nude mice for established intracranial gliomas when the tumor emitted 10^5–10^6 psc in a randomized fashion (each group had tumors of similar size, average tumor emitted 5×10^5 psc at time of treatment). Tumors typically reached this size 2 to 3 weeks after inoculation with luciferase-stable U87 MG cells into the striatum. Due to volume limitations using linear PEI in the mouse brain, we reduced the dose of plasmid used to inject sc tumors from 20 (in 100 μl) to 2.5 μg (in 5 μl) for use in intracranial tumors. We administered empty vector or statin-AE/sFlt-1 transposon vectors, with or without SB-transposase-encoding DNA, into intracranial gliomas by slow infusion with a micropump over 20 min. Identical injections were repeated 1 week later.

To verify gene transfer to intracranial gliomas, we euthanized several mice 48 h after a single plasmid injection and conducted immunostaining on brain sections using an anti-His antibody (sFlt-1 has a His tag on its C-terminus). We observed specific staining for sFlt-1 in intracranial tumors that had been injected with sFlt1, but no significant staining in empty vector-treated controls (Fig. 6A). Examining sections from five different brains injected with sFlt-1 or empty vector revealed that the transfected cells were localized mainly in the tumor itself, with rare sFlt-1-positive cells observed in the normal brain near the tumor–brain border (Fig. 6A). Similar results were obtained using an anti-HA antibody in brains injected with statin-AE-encoding plasmid; statin-AE-positive cells were localized mainly in the tumor (statin-AE is HA tagged, not shown). These results demonstrate that convection-enhanced delivery of plasmid DNA/PEI complexes transfects intracranial human glioma cells. We imaged the remaining plasmid-treated mice for luciferase activity *in vivo* every week and monitored them for survival. A light intensity of 10^7 psc consistently indicated that the death of the animal would occur within 1 week. By 3 weeks after the first plasmid administration, only 20% (2/10) of empty vector-treated mice were alive. In contrast, when we treated tumors with statin-AE/sFlt-1 vectors, 50% (4/8) of non-SB-treated mice and 73% (8/11) of SB-treated mice were alive (Fig. 6B). By 6 weeks after the first plasmid injection, all mice had died due to tumor burden, except for 2/11 (18%) SB-treated mice that no longer had any detectable tumor by luciferase *in vivo* imaging. These mice appeared to be cured of tumor, similar to what we observed with a sixfold greater dose of plasmid introduced into sc gliomas (Figs. 4A–4D). Coadministration of SB-transposase-encoding DNA provided a significant increase in animal survival relative to empty vector by log rank (Mantel–Cox) statistical analysis ($P = 0.008$). In contrast, mice treated with statin-AE/sFlt-1 without co-

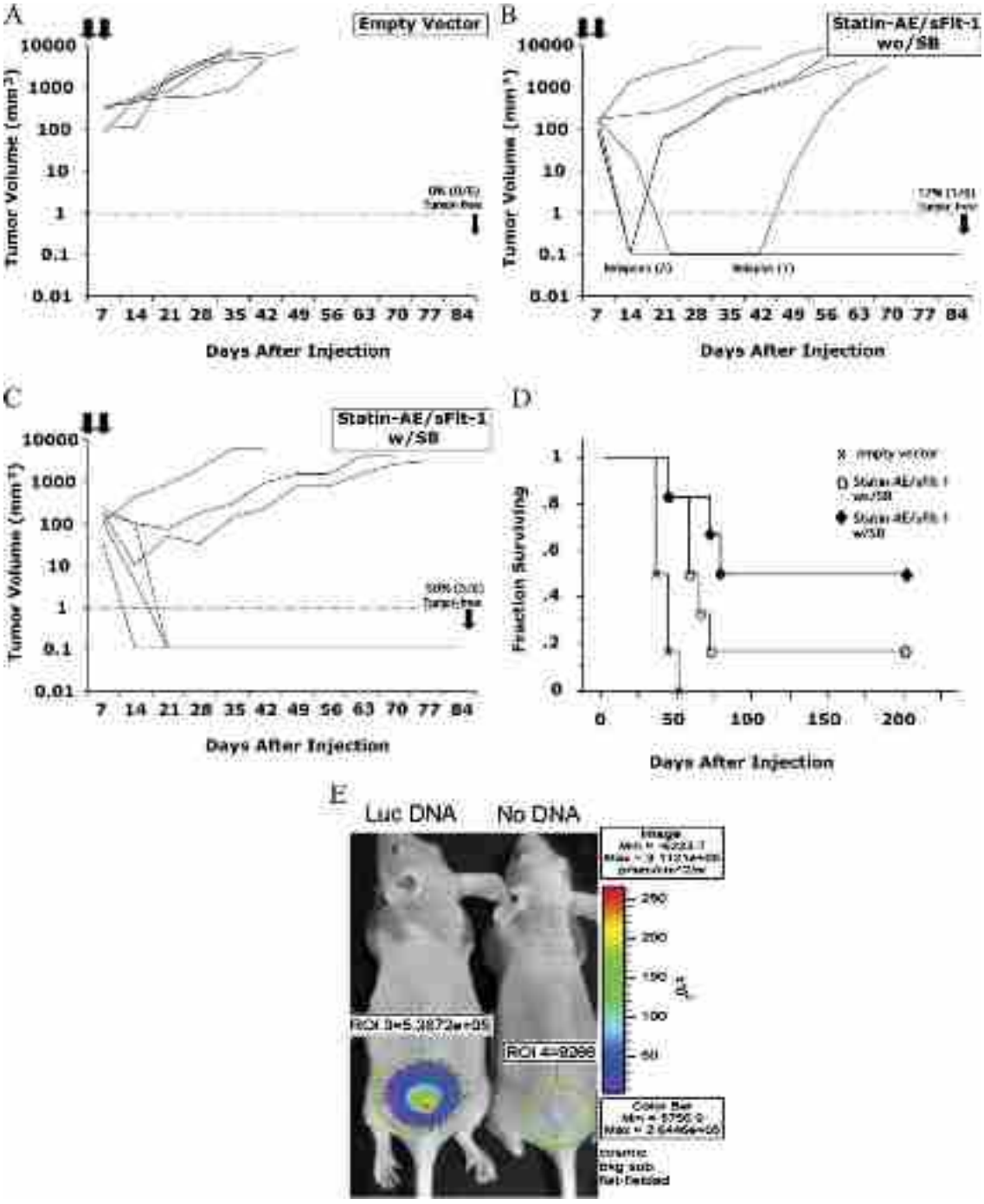

FIG. 4. Nude mice bearing subcutaneous tumors were treated with two intratumoral co-injections of 5 μg of pT2/CLUC with 15 μg of (A) pT2/CAG, (B) pT2/CFlt-1 and pT2/CAE (7.5 μg each), or (C) pT2/CFlt-1//PGK-SB and pT2/CAE//PGK-SB (7.5 μg each) ($n = 6$/group). Plasmid injections were administered on day 0 and day 3 (arrows indicate injections). Each line represents the measured tumor size of one mouse. Tumors that regressed to a size invisible to the naked eye are plotted below the dotted line as ''tumor-free.'' Tumors that regrew after nearly complete regression are marked in (B) as relapses. (D) Cumulative survival of the animals in (A–C). (E) Nude mice bearing subcutaneous tumors from (A–C) were imaged *in vivo* for luciferase activity 48 h after two injections of 5 μg pT2/CLUC/PEI complex. One representative mouse that was injected is shown on the left. An uninjected control is shown on the right (No DNA), indicating that the background level of measured luciferase activity is roughly 9000 photons/s/cm^2 in this experiment.

doi:10.1016/j.ymthe.2005.07.689

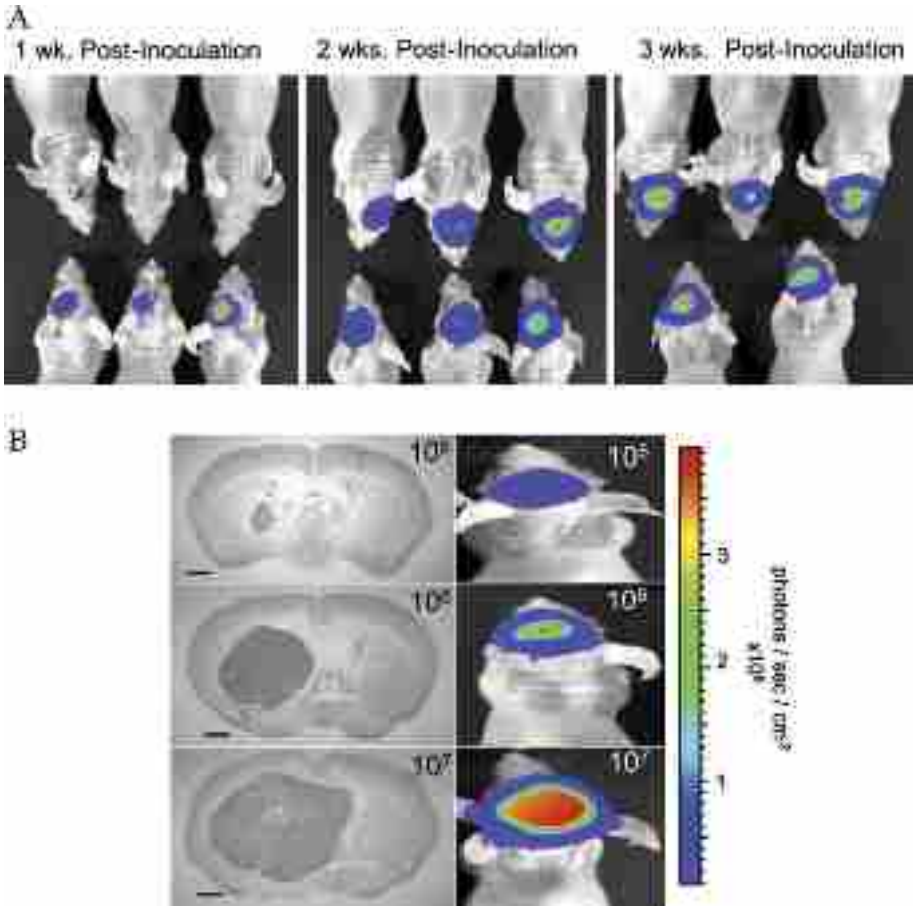

FIG. 5. (A) Nude mice bearing intracranial U87 MG luciferase-stable tumors were imaged *in vivo* for luciferase activity at 1, 2, and 3 weeks after tumor cell implantation. Five or six of 30 representative mice are shown at each time point; the images do not show the exact same mice over time. (B) Nude mice bearing intracranial U87 MG luciferase-stable tumors were imaged *in vivo* for luciferase activity. Mice were euthanized to conduct histological analysis on the tumors when measured luciferase activity was at 1×10^5, 1×10^6, and 1×10^7 photons/s/cm^2 (psc; $N = 3$/condition). A representative tumor is shown (left), which corresponds with the light emitted (right) as measured by luciferase *in vivo* imaging. A light intensity of 10^5 psc corresponded to a tumor that was approximately 1 mm^3 ($\pm$0.5) in volume, 10^6 psc to 30 mm^3 ($\pm$9) in volume, and 10^7 psc to 74 mm^3 ($\pm$17) in volume. Scale bar, 1 mm.

injection of SB-transposase-encoding DNA did not survive significantly longer than empty vector-treated controls ($P = 0.26$; Fig. 6C). These data demonstrate that SB improves the efficacy of nonviral antiangiogenic gene therapy vectors against established intracranial gliomas by providing long-term anti-tumor activity.

DISCUSSION

Antiangiogenesis therapy for cancer received a great deal of attention in the 1990s when molecules such as endostatin cured tumor xenografts when administered as a recombinant protein [34]. The appeal of such an approach was that it was nontoxic, noninvasive, and extremely effective in a mouse model. However, the phase I clinical trial for endostatin was disappointing because little, if any, tumor stabilization resulted [9]. Subsequent studies have suggested that for optimal efficacy, the inhibitor must be continuously present to offset constant secretion of proangiogenic stimulus [35–37]. Thus, supplying the inhibitor long term by gene transfer technologies should increase clinical efficacy; the results obtained in this study support this hypothesis. An additional consideration is the identification of the most potent angiogenesis inhibitor to optimize the anti-tumor effect. Comparative analysis of antiangiogenic molecules has been conducted by gene transfer in a sc model [26] and using cell-based vectors in an intracranial model [7]. Both studies showed that endostatin was not as effective as other inhibitors such as sFlt-1 [26] or interferon-α [7], clearly indicating that the choice of inhibitor is important. However, gliomas are inherently difficult to treat due to their invasive nature, heterogeneity, and ability to become resistant

FIG. 6. (A) Mice bearing intracranial luciferase-stable U87 MG tumors were intratumorally injected with 2.5 μg of pT2/CFlt-1 DNA/PEI complexes and 2 days later the brains were removed for sFlt-1 immunofluorescent staining. SFlt-1-postive cells are red; the tumor is marked by closely situated nuclei with DAPI (blue). Scale bar, 1 mm. (B) Mice bearing intracranial luciferase-stable U87 MG tumors were intratumorally injected with 2.5 μg of pT2/CFlt-1 and pT2/CAE ($N = 8$; 1.25 μg/each) or pT2/CFlt-1//PGK-SB and pT2/CAE//PGK-SB ($N = 11$; 1.25 μg/each) or 2.5 μg of empty vector ($N = 10$) DNA/PEI complexes. An identical injection was repeated 1 week later. Mice were imaged in vivo until death occurred from tumor burden; representative mice are shown (left) and the percentage of living animals/time is shown (right). (C) Cumulative survival of animals from (B).

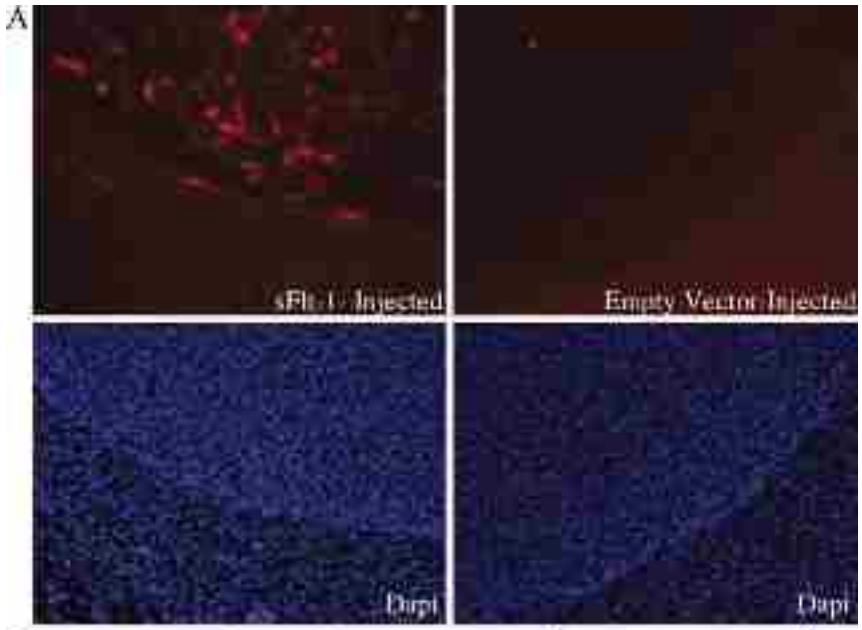

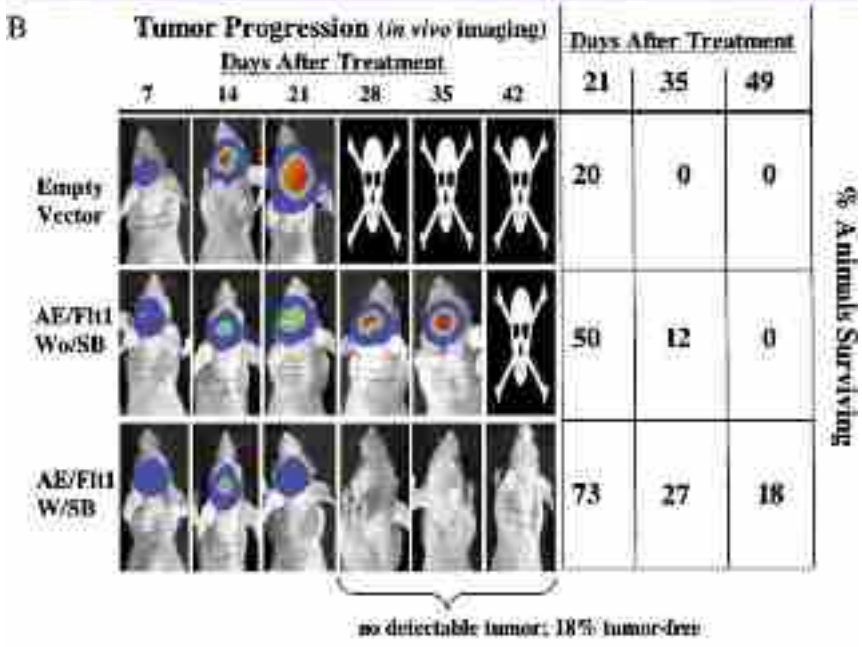

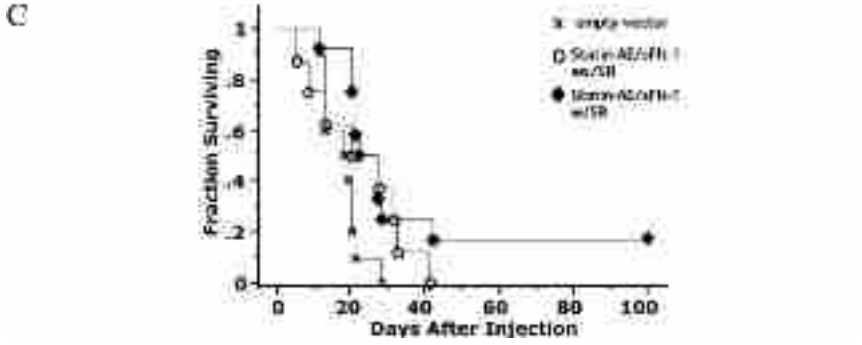

doi:10.1016/j.ymthe.2005.07.689

to monotherapies [reviewed in 4]. Therefore, it is less likely that any single inhibitor of angiogenesis (or any drug) will provide a long-term remedy for human GBM.

In this study, we found that stable coexpression of statin-AE and sFlt-1 in human glioma cells abolished the ability of these cells to form tumors, whereas expression of either protein alone only inhibited tumor growth (Fig. 3). In addition, complete tumor regression by gene transfer was achieved only when statin-AE and sFlt-1 transposons were co-injected (compare Fig. 2A with Fig. 4C). Thus, it is likely that sFlt-1 and statin-AE work additively and/or synergistically to inhibit tumor growth, by inhibiting tumor-induced angiogenesis together more effectively than as single proteins. This would not be surprising because sFlt-1 acts as a dominant negative VEGF receptor, thereby decreasing the concentration of an endothelial mitogen available to bind its signaling receptor [25,29,38–40], whereas angiostatin and endostatin can have direct anti-tumor effects, in addition to inhibiting endothelial cell growth and migration [7,35,36,41–43]. This approach is promising, but further study is needed to maximize and refine the combinatorial effect. Perhaps a cocktail of several antiangiogenic, immunostimulatory, and/or tumor-targeted suicide genes could work in concert to abolish human GBM. In support of this, several studies have shown that combining angiogenic inhibitors with suicide genes by viral gene transfer enhances their anti-tumor effect in animal models [35,44].

This is the first demonstration that a nonviral vector can increase survival and induce sustained tumor regression in an established glioma by *in situ* antiangiogenic gene transfer. Although viral vectors have been preferentially applied against experimental GBM models, nonviral vectors offer several advantages. Such vectors are simpler, more amenable to large-scale manufacture, and potentially safer (risk of replication eliminated, inflammatory response potentially reduced). We previously reported that SB mediates transgene integration and long-term expression of reporter genes in xenografted human glioblastoma [18]. Accordingly, we hypothesized that SB could increase the efficacy of nonviral cancer gene therapy vectors by facilitating long-term expression of genes that inhibit tumor growth, thereby overcoming the problem of transient expression using plasmids.

In this study we demonstrated that including SB-transposase-encoding DNA on the same molecule as the antiangiogenic transposon facilitated long-term inhibition of tumor growth. Codelivery of SB-transposase-encoding DNA with statin-AE and sFlt-1 transposons resulted in higher long-term survival than without coadministration of SB (Figs. 4D and 6C). In addition, coadministration of SB-transposase-encoding DNA resulted in the highest level of sustained tumor regression; 50% of statin-AE/sFlt-1/SB-treated animals were rendered tumor-free using the subcutaneous U87 tumor model and 18% using the intracranial U87 model (Figs. 4C and 6B). These data support the hypothesis that SB-mediated gene transfer increases the efficacy of nonviral cancer gene therapy vectors.

Previous studies have shown that gene therapy for experimental gliomas can have significant anti-tumor effects and improve long-term survival [reviewed in 4]. However, treatment for experimental gliomas is often administered less than 1 week after tumor cell implantation, when the tumor may be very small and not representative of an appreciable human glioma. We found that experimental intracranial gliomas grew at different rates, sometimes taking 3 weeks to develop into a large glioma. To overcome this variability we developed a luciferase-stable human glioblastoma cell line that can be used to quantify tumor burden by luciferase *in vivo* imaging and we began treatment when large, established gliomas of comparable sizes were present.

The decrease in efficacy observed in the intracranial model relative to the sc model (compare Figs. 4D and 6C) might be due to the sixfold decrease in plasmid dose, which was adjusted for volume of the mouse brain. Such volume adjustments may not be necessary in a large animal model or human patient. In addition, intracranial plasmid administration was done by stereotactic injection into the same location where the tumor was implanted. It would be optimal to use real-time imaging of the tumor at the time of plasmid administration to ensure ideal vector placement. Developing novel infusion catheters, better chemical conjugates, potent combinations of anti-tumor genes, and improved SB transposon vectors should increase the efficacy of nonviral gene therapy against GBM. In addition, future studies should assess if repeated administrations of therapeutic plasmids are able to increase anti-tumor efficacy.

Over the past 2 decades gene therapy for GBM has been rigorously investigated and has shown promise in animal models. Clinical efficacy was recently demonstrated in a randomized phase III clinical trial using adenoviral vectors to deliver herpes simplex virus thymidine kinase, followed by intravenous administration of ganciclovir; mean survival was nearly doubled [45]. Delivering secreted inhibitors of angiogenesis has the potential to improve the prognosis for GBM because the inhibitor can diffuse away from the producer cells, thereby spreading the anti-tumor effect. In related studies, we have found the glial cells are transfected with the luciferase gene when DNA/PEI complexes are injected into the striatum of mice without tumors (data not shown). Transfection of normal cells with anti-angiogenic genes may have contributed to the long-term anti-tumor effect of SB due to continuous secretion of inhibitor. However, the consequences of long-term expression of antiangiogenic genes in normal brain cells

warrants further study and might require regulatable gene expression systems. Clinically, antiangiogenic gene therapy for GBM may be most useful as an adjuvant therapy after surgery/radiation, to prevent regrowth of migratory glioma cells that have escaped surgical resection. SB offers a novel, nonviral method to achieve therapeutic levels of gene transfer in human GBM-derived tumors. SB could be used to augment conventional therapy for GBM or other cancers, by achieving long-term expression of proteins that inhibit tumor growth. As gene transfer technologies for GBM are improved and combination strategies are optimized, an increase in clinical efficacy will likely follow.

Materials and Methods

Plasmid DNA, PEI, and cell lines. Human glioblastoma-derived cell lines U373 MG and U87 MG were kindly provided by Dr. Daniel Vallera (University of Minnesota, Minneapolis, MN, USA). All cell lines were grown in DMEM (Gibco) supplemented with 10% heat-inactivated FBS, 1% penicillin/streptomycin, and 1% NEAA. Linear 22-kDa polyethylenimine (ExGen 500) was purchased from Fermentas (Lithuania).

The murine soluble Flt-1 cDNA was a kind gift from Dr. Richard Mulligan (Harvard University, Boston, MA, USA) and has been described previously [26]. Statin-AE is an angiostatin–endostatin fusion gene consisting of the murine fragments of plasminogen and collagen XVIII and has been described previously [13]. pCMVSB and pT2C/Luc have been described previously [18]. Statin-AE and sFlt-were cloned into pT2/CAG [46] as an *Eco*RI/*Bgl*II fragment to generate pT2/CAE and pT2/CFlt-1, respectively. pT2/CAE/BSD was made by ligating a blasticidin-resistance gene into pT2/CAE as an *Ssp*I fragment. pT2/CFlt-1/Hygro was made by ligating a hygromycin B-resistance gene into pT2/CFlt-1 as a *Bam*HI fragment. pT2/C-BSD and pT2/C-Hygro are "empty vector" controls generated by cutting out the statin-AE or sFlt-1 cDNA from pT2/CAE/BSD or pT2/CFlt-1/Hygro as a *Pme*I/*Sna*BI fragment and religating. All stable clones described in Fig. 3 were generated by transfection of the indicated plasmids (see figure legend) and drug selection in 1 μg/ml blasticidin, 20 μg/ml hygromycin B, or both drugs simultaneously. A phosphoglycerate kinase (PGK)-regulated SB transposase cassette [18] was ligated into pT2/CAE and pT2/CFlt-1 as a *Bsa*I/*Pme*I fragment to generate pT2/CAE//PGK-SB and pT2/CFlt-1//PGK-SB, respectively. Clinical-grade plasmid DNA was used in all animal studies and was prepared by Nature Technologies (Lincoln, NE, USA) at a concentration of 2 μg/μl in 0.1× buffer TE.

Tumor inoculations, intratumoral plasmid injections, size measurements, and volume calculations. Female BALB/c homozygous (nu/nu) mice, 6–8 weeks of age, were maintained in a specific-pathogen-free facility according to the guidelines of the University of Minnesota Animal Care and Use Committee. For the sc tumor model, animals were inoculated by sc injection with GBM-derived cell line U373 (5×10^6) or U87 (3.5×10^6). One to three weeks after inoculation the tumors were 5–10 mm in diameter and were injected with 100 μl of DNA/PEI complexes (N/P ratio = 7) in 5% glucose into all four tumor quadrants with a syringe (100 μl in 60 s). Tumor size was measured at regular intervals using a pair of calipers and the tumor volume (mm^3) was calculated by the product of $L \times W \times H$ of the measured tumor. For intracranial tumor inoculations and gene delivery, animals were deeply anesthetized with a ketamine/xylazine cocktail solution (53.7 mg/ml ketamine, 9.26 mg/ml xylazine) delivered at 1 ml/kg. After the animal was secured in a stereotaxic frame, 1.5 μl of luciferase-stable U87 glioma cell suspension (750,000 cells in PBS) was injected into the left striatum (+0.5 AP, 1.8 ML, −2.5 DV from bregma). For gene delivery, animals were secured in a stereotaxic frame as described above. Convection-enhanced delivery was performed through the use of a 10-μl syringe (Hamilton Model 701) and an infusion pump (Carnegie Medicin Model 100) to deliver 2.5 μg of DNA/PEI in 5 μl of 5% dextrose solution into the tumor mass over a 20-min period (0.25 μl/min). Intracranial tumor volume was estimated as follows: 30-μm serial sections were selected at a one in six interval and stained to visualize tumor mass. Images were captured and tumor area per section was measured using ImageJ software. The area measurement was used to calculate tumor volume per section and the estimated total tumor volume.

Brain histology and immunostaining. Thirty-micrometer coronally cut sections were stained for sFlt-1 and statin-AE. We used rabbit anti-HA from QED Biosciences, Inc. (San Diego, CA, USA) (1:500) to detect sFlt-1 and Chemicon's (Temecula, CA, USA) rabbit anti-His antibody (1:1000) for statin-AE. The secondary antibody used for fluorescence detection was donkey anti-rabbit IgG PE from Santa Cruz Biotechnology (Santa Cruz, CA, USA) The tissue sections were washed with sterile PBS and blocked with normal goat serum. The primary antibodies were applied to the sections and were incubated overnight on an orbital shaker at 4°C. The secondary antibody was added the following day for an hour at room temperature. The sections were then mounted on a slide using Vector Lab's Vectashield mounting medium with DAPI. The slides were allowed to dry (protected from light) and viewed on the Zeiss Apotome microscope. Pictures were captured at 10× magnification using Axiovision software according the manufacturer's instructions.

Histological analysis of intracranial tumors was conducted by Nissl staining; sections were mounted on slides and allowed to dry on a slide warmer. Slides were placed in cresyl violet solution for 3–5 min to achieve the desired stain. Dehydration was achieved through 30-s successive washes in 50, 70, and 95% EtOH and then xylene. Tissue was allowed to dry and then coverslips were applied using DPX mounting media.

CD31/PECAM-1 immunohistochemistry and vessel density assay. Tumor samples were embedded in OCT and snap frozen in preparation for cryosectioning. Immunohistochemical detection was performed on 5- to 10-μm sections, using primary antibody against PECAM-1 (R&D Systems, Minneapolis, MN, USA; BBA7, 1:1000–1:5000 of a 1 mg/ml stock solution) and anti-mouse IgG (whole molecule) peroxidase conjugate (A9044; Sigma). The staining was visualized using the cell and tissue staining kit (HRP/DAB anti-mouse, CTS002) obtained from R&D Systems. The microvessel density was calculated as the average number of PECAM (CD-31)-stained microvessels within three microscopic fields containing the maximum number of discrete microvessels, usually at the tumor periphery (as previously described [47]).

Transfections, stable cell lines, and ELISA. Human GBM-derived U373 MG cells (1×10^6) were seeded in 10-cm dishes and transfected with 5 μg of plasmid DNA using Mirus LT1 transfection reagent (Mirus, Madison, WI, USA). Culture supernatant and cell lysates were collected; lysates were collected by lysing adherent cells with luciferase lysate buffer (Promega, Madison, WI, USA). Fifty microliters of supernatant and cell lysate was used in an endostatin and Flt-1 ELISA (Chemicon International and R&D Systems, respectively); ELISA was performed according to the manufacturer's instructions. Statin-AE-transfected cells served as a negative control for Flt-1 ELISA, and sFlt-1-transfected cells served as a negative control for the endostatin ELISA. Stable GBM-derived U373 cell lines were generated by transfection with the indicated plasmids (Fig. 3 legend) and selection in 1 μg/ml blasticidin, 20 μg/ml hygromycin B, or both drugs at once (Invitrogen, San Diego, CA, USA). Stable clones were then pooled for use in experiments. The luciferase-stable cell line was generated by transfecting 100,000 U87 MG cells with 5 μg of pLUC-BSD using Mirus LT1 transfection reagent (Mirus), selecting in 1 μg/ml blasticidin for 2 weeks, and assaying blasticidin-resistant clones for luciferase activity. The clone with the highest level of luciferase activity was then plated out at limiting dilution and a single clone was isolated again and verified for luciferase activity (to ensure a true clonal population).

Luciferase in vivo imaging and analysis. Nude mice were deeply anesthetized by ip injection with avertin (225 mg/kg) and injected with 150 μl of luciferin (substrate for luciferase enzyme, 28.5 mg/ml; Xenogen).

doi:10.1016/j.ymthe.2005.07.689

Mice were imaged 5 min after luciferin injection. A 1-s gray-scale exposure was overlaid with a 5-min luminescent exposure taken with the Xenogen camera. Luciferase activity was analyzed using Living Image software (version 2.2; Xenogen) according to the manufacturer's instructions.

Statistical analysis. Differences between treatment groups and data sets were evaluated by two-sided Student's t test; $P \leq 0.05$ was considered significant. Differences in animal survival between treated and untreated controls (empty vector) were evaluated by log rank (Mantel–Cox) statistical analysis using 2 degrees of freedom; $P \leq 0.05$ was considered significant.

ACKNOWLEDGMENTS

These studies were conducted with grant support from the University of Minnesota Cancer Center and the Arnold Mabel Beckman Center for Transposon Research. John Ohlfest and Rachel Saplis were supported by a NIH cancer biology training grant.

RECEIVED FOR PUBLICATION MAY 16, 2005; REVISED JULY 24, 2005; ACCEPTED JULY 25, 2005.

REFERENCES

1. Glinski, B., Dymek, P., and Skolyszewski, J. (1998). Altered therapy schedules in postoperative treatment of patients with malignant gliomas: twenty year experience of the Maria Sklodowska-Curie Memorial Center in Krakow, 1973–1993. *J. Neurooncol.* **36:** 159–165.
2. Takano, S., Kamiyama, H., Tsuboi, K., and Matsumura, A. (2004). Angiogenesis and antiangiogenic therapy for malignant gliomas. *Brain Tumor Pathol.* **21:** 69–73.
3. Demuth, T., and Berens, M. E. (2004). Molecular mechanisms of glioma cell migration and invasion. *J. Neurooncol.* **70:** 217–228.
4. Lam, P. Y., and Breakefield, X. O. (2001). Potential of gene therapy for brain tumors. *Hum. Mol. Genet.* **10:** 777–787.
5. Hanahan, D., and Folkman, J. (1996). Patterns and emerging mechanisms of the angiogenic switch during tumorigenesis. *Cell* **86:** 353–364.
6. Ma, H. I., *et al.* (2002). Intratumoral gene therapy of malignant brain tumor in a rat model with angiostatin delivered by adeno-associated viral (AAV) vector. *Gene Ther.* **9:** 2–11.
7. De Bouard, S., *et al.* (2003). Antiangiogenic therapy against experimental glioblastoma using genetically engineered cells producing interferon-alpha, angiostatin, or endostatin. *Hum. Gene Ther.* **14:** 883–895.
8. Wu, J., Zhang, X., and Gao, D. (2000). [Inhibition of human glioma growth in nude mice by local secretion of angiostatin K(1-3)]. *Zhonghua Yi Xue Za Zhi* **80:** 861–864.
9. Eder, J. P., Jr., *et al.* (2002). Phase I clinical trial of recombinant human endostatin administered as a short intravenous infusion repeated daily. *J. Clin. Oncol.* **20:** 3772–3784.
10. Shepherd, F. A., and Sridhar, S. S. (2003). Angiogenesis inhibitors under study for the treatment of lung cancer. *Lung Cancer* **41**(Suppl. 1)**:** S63–S72.
11. Li, M., *et al.* (2002). Enhanced antiangiogenic therapy of squamous cell carcinoma by combined endostatin and epidermal growth factor receptor-antisense therapy. *Clin. Cancer Res.* **8:** 3570–3578.
12. Scappaticci, F. A., *et al.* (2001). Combination angiostatin and endostatin gene transfer induces synergistic antiangiogenic activity *in vitro* and antitumor efficacy in leukemia and solid tumors in mice. *Mol. Ther.* **3:** 186–196.
13. Scappaticci, F. A., *et al.* (2001). Statin-AE: a novel angiostatin-endostatin fusion protein with enhanced antiangiogenic and antitumor activity. *Angiogenesis* **4:** 263–268.
14. Bello, L., *et al.* (2004). Combinatorial administration of molecules that simultaneously inhibit angiogenesis and invasion leads to increased therapeutic efficacy in mouse models of malignant glioma. *Clin. Cancer Res.* **10:** 4527–4537.
15. Montemurro, F., Valabrega, G., and Aglietta, M. (2004). Trastuzumab-based combination therapy for breast cancer. *Expert Opin. Pharmacother.* **5:** 81–96.
16. Kaubisch, A., Kaleya, R., Haynes, H., Rozenblit, A., and Wadler, S. (2004). Phase II clinical trial of parenteral hydroxyurea in combination with fluorouracil, interferon and filgrastim in the treatment of advanced pancreatic, gastric and neuroendocrine tumors. *Cancer Chemother. Pharmacol.* **53:** 337–340.
17. Rigas, J. R. (2004). Taxane–platinum combinations in advanced non-small cell lung cancer: a review. *Oncologist* **9**(Suppl. 2)**:** 16–23.
18. Ohlfest, J. R., Lobitz, P. D., Perkinson, S. G., and Largaespada, D. A. (2004). Integration and long-term expression in xenografted human glioblastoma cells using a plasmid-based transposon system. *Mol. Ther.* **10:** 260–268.
19. Ivics, Z., Hackett, P. B., Plasterk, R. H., and Izsvak, Z. (1997). Molecular reconstruction of Sleeping Beauty, a Tc1-like transposon from fish, and its transposition in human cells. *Cell* **91:** 501–510.
20. Izsvak, Z., Ivics, Z., and Plasterk, R. H. (2000). Sleeping Beauty, a wide host-range transposon vector for genetic transformation in vertebrates. *J. Mol. Biol.* **302:** 93–102.
21. Ohlfest, J. R., *et al.* (2005). Phenotypic correction and long-term expression of factor VIII in hemophilic mice by immunotolerization and nonviral gene transfer using the Sleeping Beauty transposon system. *Blood* **105:** 2691–2698.
22. Yant, S. R., Meuse, L., Chiu, W., Ivics, Z., Izsvak, Z., and Kay, M. A. (2000). Somatic integration and long-term transgene expression in normal and haemophilic mice using a DNA transposon system. *Nat. Genet.* **25:** 35–41.
23. Yant, S. R., Ehrhardt, A., Mikkelsen, J. G., Meuse, L., Pham, T., and Kay, M. A. (2002). Transposition from a gutless adeno-transposon vector stabilizes transgene expression in vivo. *Nat. Biotechnol.* **20:** 999–1005.
24. Montini, E., *et al.* (2002). In vivo correction of murine tyrosinemia type I by DNA-mediated transposition. *Mol. Ther.* **6:** 759–769.
25. Yoshimura, I., Mizuguchi, Y., Miyajima, A., Asano, T., Tadakuma, T., and Hayakawa, M. (2004). Suppression of lung metastasis of renal cell carcinoma by the intramuscular gene transfer of a soluble form of vascular endothelial growth factor receptor I. *J. Urol.* **171:** 2467–2470.
26. Kuo, C. J., *et al.* (2001). Comparative evaluation of the antitumor activity of antiangiogenic proteins delivered by gene transfer. *Proc. Natl. Acad. Sci. USA* **98:** 4605–4610.
27. Niwa, H., Yamamura, K., and Miyazaki, J. (1991). Efficient selection for high-expression transfectants with a novel eukaryotic vector. *Gene* **108:** 193–199.
28. Kootstra, N. A., Matsumura, R., and Verma, I. M. (2003). Efficient production of human FVIII in hemophilic mice using lentiviral vectors. *Mol. Ther.* **7:** 623–631.
29. Ye, C., *et al.* (2004). sFlt-1 gene therapy of follicular thyroid carcinoma. *Endocrinology* **145:** 817–822.
30. De, A., Lewis, X. Z., and Gambhir, S. S. (2003). Noninvasive imaging of lentiviral-mediated reporter gene expression in living mice. *Mol. Ther.* **7:** 681–691.
31. Moriuchi, S., *et al.* (2002). Double suicide gene therapy using a replication defective herpes simplex virus vector reveals reciprocal interference in a malignant glioma model. *Gene Ther.* **9:** 584–591.
32. Ali, S., *et al.* (2004). Inflammatory and anti-glioma effects of an adenovirus expressing human soluble Fms-like tyrosine kinase 3 ligand (hsFlt3L): treatment with hsFlt3L inhibits intracranial glioma progression. *Mol. Ther.* **10:** 1071–1084.
33. Rehemtulla, A., *et al.* (2000). Rapid and quantitative assessment of cancer treatment response using in vivo bioluminescence imaging. *Neoplasia* **2:** 491–495.
34. O'Reilly, M. S., *et al.* (1997). Endostatin: an endogenous inhibitor of angiogenesis and tumor growth. *Cell* **88:** 277–285.
35. Ma, H. I., *et al.* (2002). Suppression of intracranial human glioma growth after intramuscular administration of an adeno-associated viral vector expressing angiostatin. *Cancer Res.* **62:** 756–763.
36. Griscelli, F., *et al.* (1998). Angiostatin gene transfer: inhibition of tumor growth in vivo by blockage of endothelial cell proliferation associated with a mitosis arrest. *Proc. Natl. Acad. Sci. USA* **95:** 6367–6372.
37. Kisker, O., *et al.* (2001). Continuous administration of endostatin by intraperitoneally implanted osmotic pump improves the efficacy and potency of therapy in a mouse xenograft tumor model. *Cancer Res.* **61:** 7669–7674.
38. Heidenreich, R., *et al.* (2004). Inhibition of solid tumor growth by gene transfer of VEGF receptor-1 mutants. *Int. J. Cancer* **111:** 348–357.
39. Hoshida, T., *et al.* (2002). Gene therapy for pancreatic cancer using an adenovirus vector encoding soluble flt-1 vascular endothelial growth factor receptor. *Pancreas* **25:** 111–121.
40. Kou, B., *et al.* (2004). In vivo inhibition of tumor angiogenesis by a soluble VEGFR-2 fragment. *Exp. Mol. Pathol.* **76:** 129–137.
41. Hajitou, A., *et al.* (2002). The antitumoral effect of endostatin and angiostatin is associated with a down-regulation of vascular endothelial growth factor expression in tumor cells. *FASEB J.* **16:** 1802–1804.
42. Shichiri, M., and Hirata, Y. (2001). Antiangiogenesis signals by endostatin. *FASEB J.* **15:** 1044–1053.
43. Dkhissi, F., *et al.* (2003). Endostatin exhibits a direct antitumor effect in addition to its antiangiogenic activity in colon cancer cells. *Hum. Gene Ther.* **14:** 997–1008.
44. Pulkkanen, K. J., *et al.* (2002). The combination of HSV-tk and endostatin gene therapy eradicates orthotopic human renal cell carcinomas in nude mice. *Cancer Gene Ther.* **9:** 908–916.
45. Immonen, A., *et al.* (2004). AdvHSV-tk gene therapy with intravenous ganciclovir improves survival in human malignant glioma: a randomised, controlled study. *Mol. Ther.* **10:** 967–972.
46. Geurts, A. M., *et al.* (2003). Gene transfer into genomes of human cells by the Sleeping Beauty transposon system. *Mol. Ther.* **8:** 108–117.
47. Vermeulen, P. B., *et al.* (1996). Quantification of angiogenesis in solid human tumours: an international consensus on the methodology and criteria of evaluation. *Eur. J. Cancer* **32A:** 2474–2484.